

## Chapter 5

# Lithogeochemistry as an exploration tool

### **5.1. Introduction**

The lithogeochemical characteristics were presented in the previous chapter of metamorphic rocks that formed from precursor rock types that suffered hydrothermal alteration at the time of sulphide mineralization in a VHMS system, as identified at Areachap and Kantienpan. In this chapter, those characteristics are used to formulate geochemical vectors that may be used in regional exploration. These vectors are applied to a regional data set to identify and prioritise anomalous areas. The geochemical vectors are based on multivariate statistical methods.

For this purpose, XRF analyses from the current work on the Areachap and Kantienpan areas in combination with analysis from the Prieska Cu-Zn deposit reported by Theart (1985) are used. This is then compared to a regional data set supplied by Kumba Resources. The objective is to identify a factor that represents the hydrothermal overprint related to the original sulphide mineralization event. Statistical methods used for this include cluster and canonical analysis. The values of the identified multivariate factors are analyzed utilizing maximum likelihood procedure to identify different sub-populations in the data set.

## **5.2. Lithogeochemical interpretation of borehole information**

A database was compiled of whole rock analyses from the three known VHMS deposits in the area. There are principally three main rock types in this data set, namely peraluminous gneiss and schist, quartzo-feldspathic gneiss, and amphibolite, based on the available petrographic descriptions of the individual samples. Three different codes are used to classify these rocks. Code “A” represents peraluminous rocks, code “B” quartzo-feldspathic gneisses, and code “C” for amphibolites.

The dominant lithogeochemical features of the alteration zones at the Areachap, Kantienpan, and Copperton ore deposits are their common peraluminous, Na and Ca depleted, and K and Mg enriched nature. The enrichment of K together with Mg may suggest that the source rock was pelitic, but that has been affected by alteration processes. An unaltered pelitic source rock will display only K-enrichment. The chemical characteristics of the alteration zone may therefore be defined as having high values of  $\text{Al}_2\text{O}_3$ , MgO, and/or  $\text{K}_2\text{O}$  and low  $\text{Na}_2\text{O}$  and CaO contents.

The quartzo-feldspathic gneissic rocks have high  $\text{SiO}_2$ ,  $\text{Na}_2\text{O}$ , and  $\text{K}_2\text{O}$  and low CaO and MgO contents. They could be subdivided into two subgroups i.e., the biotite-gneisses or leucogneisses and biotite-hornblende-gneisses. The leucogneisses are characterised by lower CaO and MgO, and higher  $\text{SiO}_2$ ,  $\text{Na}_2\text{O}$  and  $\text{K}_2\text{O}$  contents, relative to biotite-hornblende-gneisses.

In general, the amphibolites have high CaO, MgO and  $\text{Fe}_2\text{O}_3$  contents and very low  $\text{SiO}_2$ ,  $\text{K}_2\text{O}$  and  $\text{Na}_2\text{O}$  contents. Two types of amphibolites are distinguished based on the source rocks (Theart, 1985). These are ortho-amphibolites, derived from igneous basic rocks, and para-amphibolites, derived from marlstones or calcareous shales. Ortho-amphibolites have high Mg, Cr, Ni and  $\text{TiO}_2$  contents and displays a positive correlation between Mg and Cr; and Ni and  $\text{TiO}_2$  (Leake, 1964). Para-amphibolite rocks have low Cr, Ni, and  $\text{TiO}_2$  contents and show negative correlation when Mg is plotted against Cr and Ni and a low positive to slightly negative correlation between MgO and  $\text{TiO}_2$  (Leake, 1964). Only the correlation between MgO and Ni could be used here to discriminate between these

rock types, as the regional data set used in the study does not include analyses for Cr. TiO<sub>2</sub> does not show a distinct correlation with MgO in this data set.

A number of multivariate statistical methods were used to calculate geochemical factors that would distinguish these rock types. The statistical methods include principal component analysis (Rao, 1964; Morrison, 1976), principal factor analysis (Mardia et al., 1979; Geweke et al., 1980) and canonical correlation analysis (Kshirsagar, 1972; Mardia et al., 1979). The canonical correlation method provides the best discriminatory results. In the canonical correlation method, the relationships between two sets of variables are analyzed (Kshirsagar, 1972; Mardia et al., 1979). The canonical coefficients or canonical weights are coefficients of the linear combinations of variables. If the variables are not measured in the same units, the standardized coefficients could be used instead of raw coefficients. This latter technique also decreases the influence of closure effects due to the summing up of major elements to 100% (Kshirsagar, 1972; Mardia et al., 1979).

The statistical analyses were done, using SAS software (SAS<sup>®</sup> version 8.2). The input data file may include all the variables determined, but in the canonical analysis, the user determines the two sets of variables for analysis.

### **5.3. Economic element vectors of mineralization**

There are two vectors based on the economic element composition of known ore bodies in the area that may be used as vectors of mineralization (Theart, 1985; Attridge, 1986; Rossouw, 2003). Elements that characterized the two ore types present in this area include:

- a) Zn, Cu, Ba and B
- b) Ni and Cu

The first vector is related to VHMS mineralization in the region, which is the focus of the current study, whereas the second relates to the Jacomynspan type Ni-Cu mineralization described by Attridge (1986). The distributions of Zn, Cu and Ni in the regional data set

were investigated by means of the probability plot procedure (Sinclair, 1976). The anomalous subpopulations were identified and will be used in the subsequent discussion.

#### **5.4. Peraluminous, gneiss, and amphibolite factors**

It is important to utilize the known geochemical relationships between various major and trace elements during canonical multivariate analysis. Each of the two sets of variables required for canonical analysis should consist of those variables that have an underlying positive geochemical correlation with each other (Kshirsagar, 1972; Mardia et al., 1979; Tauson, 1999; Shpak et al., 2003 ). Cluster analysis is used to confirm the relationship between different variables in a data set (Harman, 1976), and this helps to separate the two sets of variables. In the following sections, various additional statistical methods are applied to the pre-defined data sets of each rock type in order to identify the two sets of variables for later use in cluster analysis.

##### **5.4.1. Peraluminous factors**

The results of cluster analysis of major and trace elements in peraluminous rocks are shown in Figure 5.1. There are two main groups in this tree diagram. The first set includes  $\text{Al}_2\text{O}_3$  (+), MgO (+),  $\text{K}_2\text{O}$  (+),  $\text{Na}_2\text{O}$  (-), CaO (-), Sr (-) and the other includes Cu (+), Zn (+), Pb (+), S (+), Ba (+). The first set consists of those oxides that are enriched or depleted in the host rocks of the ore deposit, which may now be regarded as the variables defining the peraluminous factor. Rb might be replaced by K, and Sr could be replaced by Ca. The second set comprises the ore forming elements and these may be regarded as the variables defining an ore factor.

As could be expected, it was found that the log transformed values of elements that display a strongly log normal distribution gives better results than the raw values when compared with elements displaying a normal distribution. This was done by

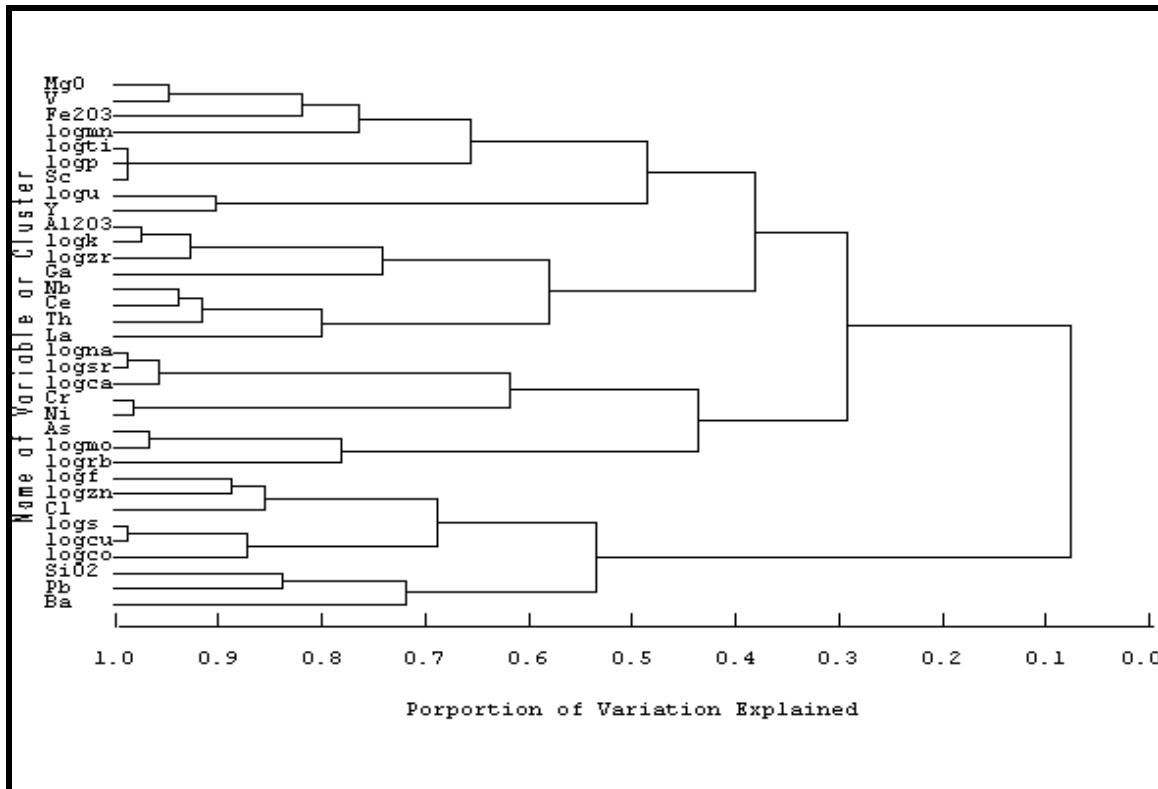


**Figure 5.1:** The tree diagram of the peraluminous rocks.

multiple inspections of the regression statistics between any two variables, and correlation coefficients.

The peraluminous factor may then be calculated by using canonical analysis of the peraluminous data set. The following factor formula was obtained:

$$F_{\text{peraluminous}} = 0.8375 * \log \text{Al}_2\text{O}_3 + 0.8877 * \log \text{Rb} + 0.7687 * \log \text{MgO} + 0.1230 * \log \text{K}_2\text{O} - 0.7069 * \text{Na}_2\text{O} - 0.5433 * \text{CaO} - 0.1923 * \log \text{Sr} = \text{FPer}$$

When this factor is applied to the combined data set of the Areachap, Kantiengan, and Copperton samples, and the results sorted, the factor values effectively separated a very high percentage (>95 %) of independently identified peraluminous samples from the combined set. However, some peraluminous samples in the Copperton data set have high CaO and/or Na<sub>2</sub>O contents and the factor failed to separate them as peraluminous.

The common pelitic rocks have high Al<sub>2</sub>O<sub>3</sub>, K<sub>2</sub>O and low MgO contents (Fig. 5.1). When the canonical analysis was applied on a data set containing samples that were independently identified as metapelitics by petrographic analysis, utilizing as first set of variables Al<sub>2</sub>O<sub>3</sub>, K<sub>2</sub>O, and Rb, which was compared to the second set containing Na<sub>2</sub>O, CaO, Sr, and MgO, the following pelitic factor is suggested:

$$F_{\text{pelitic}} = 0.8961 * \text{Al}_2\text{O}_3 + 0.2027 * \log \text{Rb} + 0.0842 * \log \text{K}_2\text{O} - 0.8675 * \text{MgO} - 0.5195 * \log \text{Na}_2\text{O} - 0.0808 * \log \text{Sr} - 0.0161 * \log \text{CaO} = \text{FPR}$$

The assumed hydrothermally altered peraluminous rocks have high Al<sub>2</sub>O<sub>3</sub> and MgO and low K<sub>2</sub>O contents (Fig. 5.1). The canonical analysis between variables Al<sub>2</sub>O<sub>3</sub>, Fe<sub>2</sub>O<sub>3</sub>, and MgO with K<sub>2</sub>O, CaO, Na<sub>2</sub>O, Rb, and Sr gives the following alteration factor:

$$F_{\text{Alteration}} = 1.1113 * \text{Al}_2\text{O}_3 + 0.2169 * \text{Fe}_2\text{O}_3 + 0.1707 * \text{MgO} - 0.8618 * \log \text{K}_2\text{O} - 0.3372 * \log \text{CaO} - 0.1913 * \log \text{Rb} - 0.1443 * \log \text{Sr} - 0.0951 * \log \text{Na}_2\text{O} = \text{FAR}$$

It is suggested that samples displaying high values for both the peraluminous and alteration factors should be prioritized as probably related to a massive sulphide bearing lithological unit.

#### 5.4.2. Gneiss factors

A cluster analysis was done of the quartzo-feldspathic gneiss data set to determine the relationship between major element oxides and trace elements (Fig. 5.2). This analysis highlights the two different rock types in the data set. One subgroup of data set has high SiO<sub>2</sub>, Na<sub>2</sub>O and K<sub>2</sub>O contents whereas the other has high MgO, CaO, Fe<sub>2</sub>O<sub>3</sub>, Cr and Ni contents. These two types of gneisses may also be identified in the tree diagram (Fig. 5.2). Rocks with high SiO<sub>2</sub>, Na<sub>2</sub>O, and K<sub>2</sub>O and low CaO, MgO, and Fe<sub>2</sub>O<sub>3</sub> contents might be classified as leuco-gneisses and the other type is the biotite-hornblende-gneiss. The general canonical factor obtained for the entire gneiss data set is:

$$F_{\text{Gneiss}} = 0.8896 * \text{SiO}_2 + 0.2247 * \log \text{K}_2\text{O} + 0.1753 * \text{Na}_2\text{O} - 0.3978 * \text{CaO} - 0.3714 * \log \text{MgO} - 0.3534 * \text{Fe}_2\text{O}_3$$

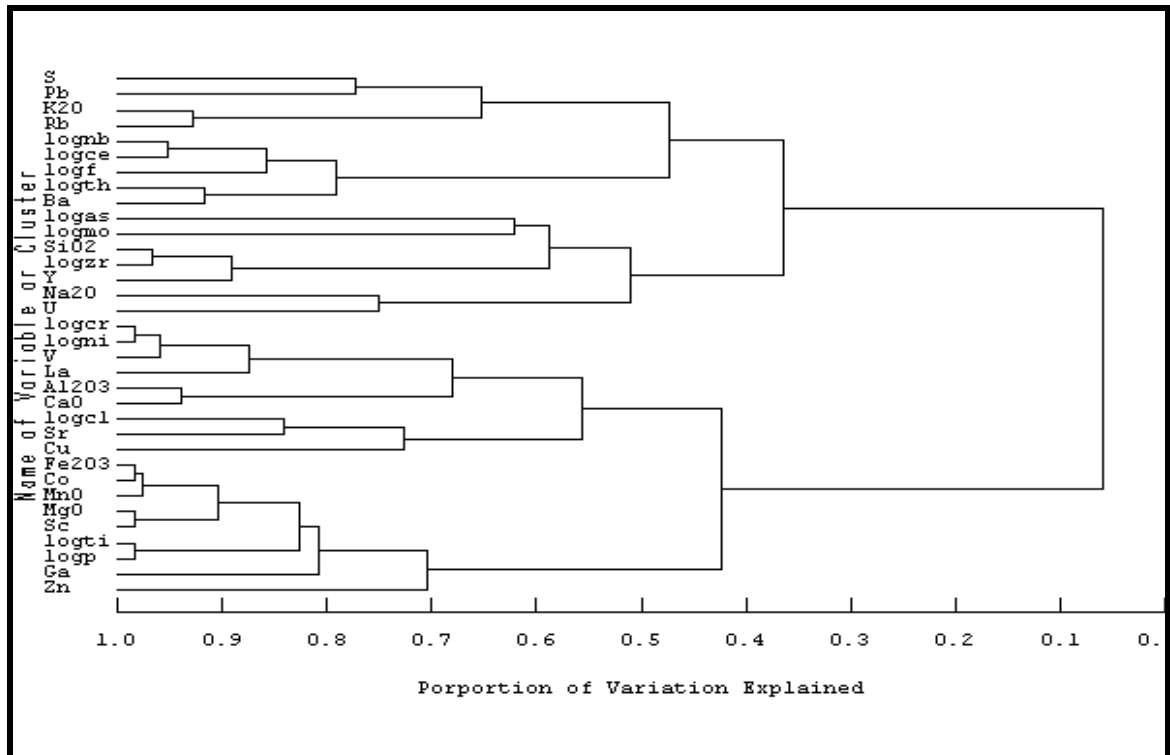


Figure 5.2: The tree diagram of the gneissic rocks.

This factor was tested using the combined data set, and it was found that some of the peraluminous samples returned high values for the gneissic factor. The reason for this is because these samples have very high SiO<sub>2</sub> (85-72%) and minor Na<sub>2</sub>O or K<sub>2</sub>O (1-2%) contents.

In the canonical analysis, where variables SiO<sub>2</sub>, Na<sub>2</sub>O, K<sub>2</sub>O, and Rb are compared with CaO, MgO, Al<sub>2</sub>O<sub>3</sub>, and Sr, the following factor for leuco-gneiss is derived:

$$F_{\text{Leu-Gn}} = 0.955 * \text{SiO}_2 + 0.1246 * \text{Na}_2\text{O} + 0.081 * \text{K}_2\text{O} + 0.0264 * \text{Rb} - 0.5633 * \text{MgO} - 0.4371 * \text{CaO} - 0.1627 * \text{Al}_2\text{O}_3 - 0.0225 * \text{Sr}$$

Canonical analysis gives the following factor for the biotite-hornblende-gneiss rocks:

$$F_{\text{Hbl-Gn}} = 0.5633 * \text{MgO} + 0.4371 * \text{CaO} + 0.1627 * \text{Al}_2\text{O}_3 + 0.0225 * \text{Sr} - 0.955 * \text{SiO}_2 - 0.1246 * \text{Na}_2\text{O} - 0.081 * \text{K}_2\text{O} - 0.0264 * \text{Rb}$$

In subsequent sections the code “B<sub>1</sub>” will be used for biotite-hornblende-gneiss.

### 5.4.3. Amphibolite factors

The results of a cluster analysis of the amphibolite data set are shown in Figure 5.3. There are good correlations between Fe<sub>2</sub>O<sub>3</sub>, TiO<sub>2</sub>, MgO, CaO, Ni, and Cr on one side and SiO<sub>2</sub>, K<sub>2</sub>O, Na<sub>2</sub>O, and Al<sub>2</sub>O<sub>3</sub> on the other side. In other words, the canonical analysis has to be calculated with a set of variables including CaO, MgO, Fe<sub>2</sub>O<sub>3</sub>, TiO<sub>2</sub>, and Ni and a set with SiO<sub>2</sub>, Al<sub>2</sub>O<sub>3</sub>, and K<sub>2</sub>O. A general amphibolite factor is then defined by:

$$F_{\text{Amphibolite}} = 0.72223 * \text{CaO} + 0.6584 * \text{Fe}_2\text{O}_3 + 0.4469 * \log \text{MgO} + 0.2729 * \text{TiO}_2 + 0.1774 * \log \text{Ni} - 0.6444 * \log \text{K}_2\text{O} - 0.4952 * \text{SiO}_2 - 0.2891 * \log \text{Al}_2\text{O}_3 - 0.2594 * \log \text{MnO}$$

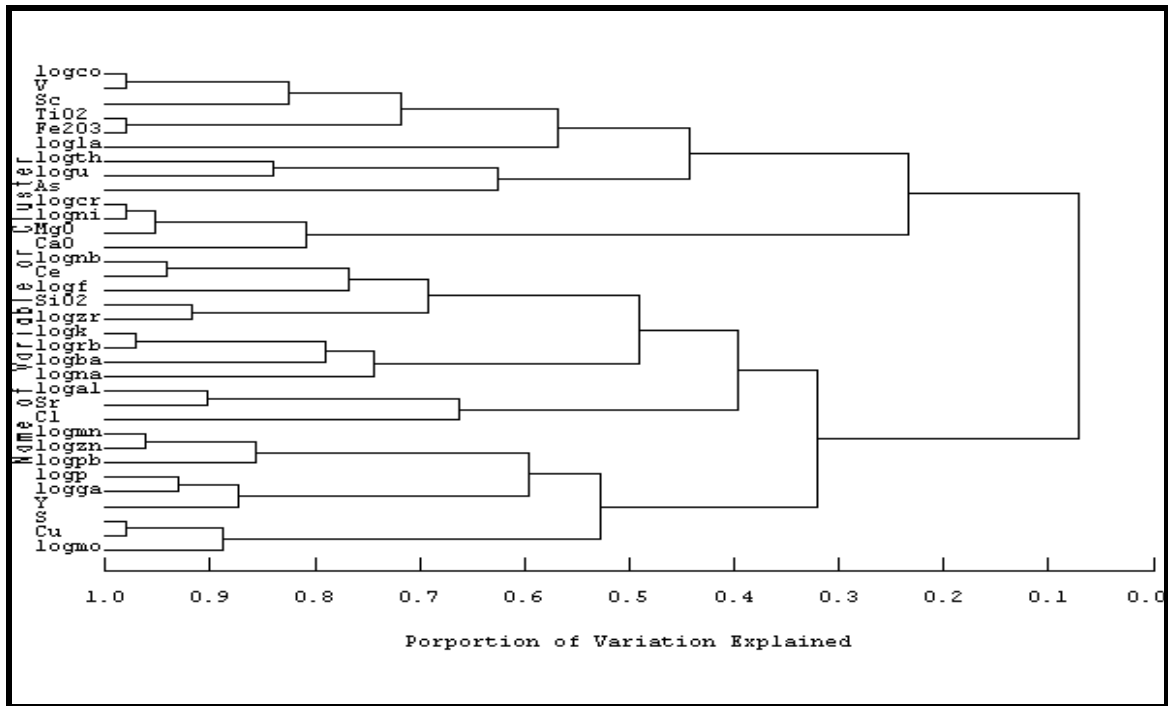


Figure 5.3: The tree diagram of the amphibolite rocks.

This factor when used for the combined data set, results in some of the gneissic samples returning high values. This may be explained by their low SiO<sub>2</sub> contents (45-54%) and low K<sub>2</sub>O contents (1-5%), and because these samples are rich in hornblende.



If a canonical analysis is done using CaO, MgO and Ni in the first set of variables and Na<sub>2</sub>O, SiO<sub>2</sub>, K<sub>2</sub>O and Rb in the second set, the following factors are derived to identify the ortho-amphibolites:

$$F_{\text{Ortho-Amp1}} = 0.6685 * \text{CaO} + 0.4981 * \text{MgO} + 0.0247 * \log \text{Ni} - 0.7536 * \log \text{Na}_2\text{O} - 0.2958 * \log \text{SiO}_2 - 0.1458 * \log \text{Rb} - 0.1177 * \log \text{K}_2\text{O}$$

$$F_{\text{Ortho-Amp2}} = 0.7588 * \text{CaO} + 0.37 * \log \text{Ni} - 0.7236 * \log \text{Na}_2\text{O} - 0.2982 * \log \text{K}_2\text{O} - 0.2399 * \log \text{SiO}_2 - 0.0008 * \log \text{Rb}$$

MgO in the para-amphibolite has a negative correlation with Ni and TiO<sub>2</sub>. The canonical factors derived for the para-amphibolite are:

$$F_{\text{Para-Amp1}} = 0.6173 * \text{CaO} + 0.5771 * \text{MgO} + 0.0756 * \text{Fe}_2\text{O}_3 - 0.5101 * \log \text{Na}_2\text{O} - 0.3706 * \log \text{Ni} - 0.2678 * \log \text{SiO}_2 - 0.2085 * \log \text{Rb} - 0.0321 * \log \text{K}_2\text{O}$$

$$F_{\text{Para-Amp2}} = 0.5619 * \text{CaO} + 0.6306 * \text{MgO} - 0.7001 * \log \text{Ni} - 0.2568 * \log \text{SiO}_2 - 0.2292 * \log \text{K}_2\text{O} - 0.2101 * \log \text{Rb}$$

$$F_{\text{Para-Amp3}} = 0.7382 * \text{MgO} + 0.439 * \text{CaO} - 0.9459 * \log \text{Ni} - 0.2358 * \log \text{TiO}_2$$

As there are some missing values for Ni in the regional data set, a general factor for amphibolite, which does not include Ni, has been derived as:

$$F_{\text{Amp2}} = 0.8404 * \text{CaO} + 0.4546 * \text{Fe}_2\text{O}_3 + 0.2584 * \log \text{MgO} + 0.196 * \log \text{TiO}_2 - 0.7205 * \log \text{K}_2\text{O} - 0.4869 * \log \text{SiO}_2 - 0.1964 * \log \text{Al}_2\text{O}_3;$$

In subsequent sections the code “C<sub>1</sub>” will be used for para-amphibolite, and the code “C<sub>2</sub>” for ortho-amphibolite.

## **5.5. Application of factors to the regional data set**

The peraluminous, alteration, and pelitic factors are the most important factors for the identification of peraluminous rocks that might be related to VHMS style alteration zones. To discriminate altered rocks from rocks containing both high MgO and K<sub>2</sub>O contents and probably had a pelitic precursor the pelitic factor values are also analysed. SAS software was used to calculate these factors for the whole regional data set. The

values calculated for each of the three factors were sorted and a maximum likelihood procedure was used to define the samples with anomalously high factor values. These samples are listed in tables below (Table 5.1, 5.2 and 5.3). Table 5.1 is sorted based on the peraluminous factor. For Table 5.2 the data is sorted based on the alteration factor, and, Table 5.3 gives anomalous samples based on the pelitic factor. The probable anomalous samples are ranked and marked by one or two stars in these tables based on their relative priority.

As shown in Table 5.1 and 5.2, samples 4, 189, 192 and 221 have the highest MgO (10.7-15 %), Al<sub>2</sub>O<sub>3</sub> (15.5-16.5 %), very low K<sub>2</sub>O (0.02-0.97 %), Na<sub>2</sub>O (0.3- 0.6 %) and CaO (0.32-0.84 %), low Ni (24-88 ppm) and slightly high Zn (177-349 ppm) contents. In these tables, there are two samples (232 and 903) with extremely high Al<sub>2</sub>O<sub>3</sub> contents (45.5-47.3 %) and high K<sub>2</sub>O contents (2.76-5.19 %), but low MgO contents (1.1-1.41 %) associated with Zn concentrations of 134 and 174 ppm respectively.

The peraluminous factor (FPer) is plotted versus alteration factor (FAR) in Figure 5.4. These two samples (232 and 903, in the first field) have the highest values for both factors. The diagram also shows seven samples that have high values for the alteration factor and these includes samples 92, 426, 430, 189,192, 221 and 222. These samples, which are located in the third field, may be related to an alteration zone.

The alteration factor (FAR) is plotted versus pelitic factor (FPR) in Figure 5.5. The same two samples (232 and 903, in the first field) have the highest values of both the alteration and pelitic factors. These samples probably represent unusual aluminous, pelitic precursors. Four samples have the highest values for the alteration factor (i.e. sample 4, 189, 192, and 221 in the third field) and lowest values for the pelitic factor. These samples are interesting in that they may represent the equivalents of rocks that were affected by ore forming alteration processes.

**Table 5.1:** Sorted data set based on the peraluminous factor (FPer) for the regional data set

No.	Code	Ranking	Al <sub>2</sub> O <sub>3</sub>	MgO	K <sub>2</sub> O	CaO	Na <sub>2</sub> O	SiO <sub>2</sub>	Cu	Zn	Ni	Ba	FPer	FPR	FAR
232	A		47.3	1.1	5.19	0.1	0.7	36.3	11	134	22	206	18.71	43.75	53.41
21	A		27.1	3.9	4.52	0.22	0.3	47.9	18	112	67	771	18.36	23.38	36.71
453	A		21.5	2.59	3.97	0.18	0.4	54.9	21	106	56	653	18.25	19.44	28.68
903	A		45.5	1.41	2.76	0.78	0.1	37.7	12	175	28	401	18.15	42.67	53.88
82	A		22.9	3.07	5.06	0.25	0.4	53.6	16	160	59	902	18.04	20.20	30.64
407	A		25.1	2.99	4.45	0.42	0.5	51.7	15	160	57	599	17.94	22.10	32.81
18	A		22.5	3.03	3.65	0.28	0.1	57.5	18	180	49	647	17.86	20.49	29.60
338	A		36.7	0.74	7.68	0.22	0.8	42.2	19	40	14	472	17.85	34.40	39.95
19	A		23.2	2.56	4.44	0.26	0.4	56.1	18	152	40	593	17.81	20.88	30.13
55	A		22.6	3.32	3.71	0.5	0.6	52.5	19	171	76	580	17.53	19.40	30.92
4	A	**	16.5	15	0.97	0.32	0.3	48.5	15	177	50	49	17.52	3.90	31.52
56	A		22.2	3.34	3.26	0.49	0.5	55.5	70	154	69	591	17.48	19.09	30.29
466	A		19.8	2.46	3.2	0.2	0.1	59.4	40	127	53	504	17.46	18.53	27.72
908	A		21.8	1.9	4.24	0.24	0.6	55.7	90	168	62	724	17.43	19.99	29.36
256	A	*	23.1	4.27	2	0.45	0.6	53	74	159	75	324	17.36	18.91	33.86
255	A	*	23.4	3.6	2.51	0.42	0.6	51.1	7	180	64	571	17.34	19.79	32.87
20	A		24.6	3.02	3.94	0.49	0.9	52.9	10	177	43	590	17.31	21.24	32.14
54	A		22.4	3.34	3.71	0.55	0.7	56.4	32	134	72	605	17.30	19.09	29.42
58	A		20.8	3.17	2.8	0.42	0.6	57.4	22	171	78	483	17.23	17.86	28.23
74	A		28.4	2.97	3.67	0.56	0.8	48.4	21	207	53	766	17.17	24.67	37.06
77	A	*	29.1	3.94	1.51	0.31	0.6	47.9	29	225	56	106	17.16	24.51	39.60
257	A	*	24.9	3.35	1.91	0.41	0.7	54.4	20	187	50	291	17.13	21.23	34.06
258	A	*	25.2	4.13	1.99	0.55	0.9	52.2	11	270	61	270	17.09	20.67	34.35
79	A		18.6	2	3.71	0.48	0.5	63.4	41	633	30	752	17.02	17.05	23.61
422	A		21	2.96	3.72	0.71	0.6	53.9	8	141	69	818	17.00	18.20	28.91
531	A		21.9	3.57	2.21	0.22	0.5	55.7	80	204	69	874	17.00	18.46	31.81
424	A		18.1	2.99	2.93	0.63	0.4	60.9	13	154	63	667	16.98	15.78	25.42
367	A		18	3.51	1.25	0.87	0.5	63.2	341	167	55	318	16.93	15.07	24.27
109	A		23.2	4.03	1.54	0.84	0.2	51.5	16	216	82	575	16.90	19.64	34.12
57	A		19.9	3.14	3.16	0.31	0.8	58.2	63	168	65	637	16.81	16.86	27.40
81	A		15.5	1.35	3.51	0.25	0.4	68.4	8	84	30	476	16.75	14.97	20.51
53	A		21.6	2.87	3.85	0.29	0.9	56.7	25	151	57	846	16.74	18.55	29.34
212	A		20	3.35	3.08	0.63	0.9	54.3	4	209	99	761	16.69	16.71	28.08
110	A		12.6	0.97	1.59	0.62	0.4	76.6	25	83	29	250	16.67	12.76	15.86
58	A		18.6	2	2.83	0.62	0.9	62.4	9	105	39	300	16.67	16.74	24.86
206	A	*	23.7	3.11	1.12	0.18	0.2	58.5	20	127	81	892	16.63	20.79	33.36
421	A		21.2	2.87	3.02	0.73	0.7	53.2	13	173	67	855	16.60	18.31	30.37
420	A		20.2	2.91	3.28	1.04	0.8	58.7	12	120	50	811	16.53	17.33	25.81
80	A		17.1	1.84	3.48	0.52	0.8	64.9	26	152	44	709	16.50	15.56	21.83
425	A		17.1	2.69	2.46	0.9	0.6	63	4	139	49	640	16.36	14.84	23.83
229	A		11.5	1.93	1.6	0.07	0.4	75.3	n.d.	77	n.d.	1131	16.06	10.73	17.77
184	A		19.5	0.46	4.45	0.15	0.7	69.3	6	81	1	1696	15.92	19.03	21.99
170	A		10.4	3.52	0.87	0.14	0.4	75.1	7	116	n.d.	806	15.80	8.16	16.90
75	A		10.6	1.15	1.89	0.43	0.5	78	18	78	27	178	15.68	10.49	13.64
172	A		9.4	2.13	1.71	0.23	0	81.7	1	49	n.d.	1354	15.67	10.43	12.06
221	A	**	16.6	10.7	0.07	0.45	0.6	45.8	14	167	88	76	15.65	6.91	36.91
192	A	**	16.2	11.7	0.24	0.43	0.3	43	17	178	24	10	15.55	6.01	37.95
426	A	*	28	4.81	0.38	0.68	0.7	44.1	46	249	94	107	15.53	22.20	43.85
189	A	**	15.5	13.7	0.23	0.84	0.6	41	12	349	25	30	15.32	3.29	36.67
92	A	*	17.3	3.03	0.19	0.68	0.2	64.3	24	137	102	2	15.20	14.83	27.15
430	A	*	24	3.63	0.25	0.57	0.5	53.7	32	190	68	87	15.10	19.74	36.75
717	A		11.7	0.27	8.37	0.26	0.8	74.8	9	11	12	1118	15.01	12.19	11.30
390	A		10.1	2.59	1.24	0.44	0.7	80.7	6	49	n.d.	215	14.99	8.36	12.78
222	A	*	13.3	2.81	0.32	0.34	0.3	69.9	12	60	3	305	14.98	11.27	23.31

Note: Ranking: anomaly ranking (\*= high to moderately high and \*\*= very high) and n.d.: Not detected

**Table 5.2:** Sorted data set based on the alteration factor (FAR) for the regional data set

No.	Code	Ranking	Al <sub>2</sub> O <sub>3</sub>	MgO	K <sub>2</sub> O	CaO	Na <sub>2</sub> O	SiO <sub>2</sub>	Cu	Zn	Ni	Ba	FAR	FPer	FPR
903	A		45.5	1.41	2.76	0.78	0.1	37.7	12	175	28	401	53.88	18.15	42.67
232	A		47.3	1.1	5.19	0.1	0.7	36.3	11	134	22	206	53.41	18.71	43.75
426	A	*	28	4.81	0.38	0.68	0.7	44.1	46	249	94	107	43.85	15.53	22.20
482	A	*	25.7	3.67	0.07	0.24	0.6	52.2	27	198	80	1	40.68	14.40	20.91
338	A		36.7	0.74	7.68	0.22	0.8	42.2	19	40	14	472	39.95	17.85	34.40
77	A	*	29.1	3.94	1.51	0.31	0.6	47.9	29	225	56	106	39.60	17.16	24.51
192	A	**	16.2	11.7	0.24	0.43	0.3	43	17	178	24	10	37.95	15.55	6.01
74	A		28.4	2.97	3.67	0.56	0.8	48.4	21	207	53	766	37.06	17.17	24.67
221	A	**	16.6	10.7	0.07	0.45	0.6	45.8	14	167	88	76	36.91	15.65	6.91
430	A	*	24	3.63	0.25	0.57	0.5	53.7	32	190	68	87	36.75	15.10	19.74
21	A		27.1	3.9	4.52	0.22	0.3	47.9	18	112	67	771	36.71	18.36	23.38
189	A	**	15.5	13.7	0.23	0.84	0.6	41	12	349	25	30	36.67	15.32	3.29
258	A	*	25.2	4.13	1.99	0.55	0.9	52.2	11	270	61	270	34.35	17.09	20.67
109	A	*	23.2	4.03	1.54	0.84	0.2	51.5	16	216	82	575	34.12	16.90	19.64
257	A	*	24.9	3.35	1.91	0.41	0.7	54.4	20	187	50	291	34.06	17.13	21.23
256	A	*	23.1	4.27	2	0.45	0.6	53	74	159	75	324	33.86	17.36	18.91
206	A	*	23.7	3.11	1.12	0.18	0.2	58.5	20	127	81	892	33.36	16.63	20.79
255	A	*	23.4	3.6	2.51	0.42	0.6	51.1	7	180	64	571	32.87	17.34	19.79
407	A		25.1	2.99	4.45	0.42	0.5	51.7	15	160	57	599	32.81	17.94	22.10
20	A		24.6	3.02	3.94	0.49	0.9	52.9	10	177	43	590	32.14	17.31	21.24
531	A	*	21.9	3.57	2.21	0.22	0.5	55.7	80	204	69	874	31.81	17.00	18.46
4	A	**	16.5	15	0.97	0.32	0.3	48.5	15	177	50	49	31.52	17.52	3.90
55	A		22.6	3.32	3.71	0.5	0.6	52.5	19	171	76	580	30.92	17.53	19.40
82	A		22.9	3.07	5.06	0.25	0.4	53.6	16	160	59	902	30.64	18.04	20.20
421	A		21.2	2.87	3.02	0.73	0.7	53.2	13	173	67	855	30.37	16.60	18.31
56	A		22.2	3.34	3.26	0.49	0.5	55.5	70	154	69	591	30.29	17.48	19.09

Note: Ranking: anomaly ranking (\*= high to moderately high and \*\*= very high)

**Table 5.3:** Sorted data set based on the pelitic factor (FPR) for the regional data set

No.	Code	Al <sub>2</sub> O <sub>3</sub>	MgO	K <sub>2</sub> O	CaO	Na <sub>2</sub> O	SiO <sub>2</sub>	Cu	Zn	Ni	Ba	FPR	FPer	FAR
232	A	47.3	1.1	5.19	0.1	0.7	36.3	11	134	22	206	43.75	18.71	53.41
903	A	45.5	1.41	2.76	0.78	0.1	37.7	12	175	28	401	42.67	18.15	53.88
338	A	36.7	0.74	7.68	0.22	0.8	42.2	19	40	14	472	34.40	17.85	39.95
74	A	28.4	2.97	3.67	0.56	0.8	48.4	21	207	53	766	24.67	17.17	37.06
77	A	29.1	3.94	1.51	0.31	0.6	47.9	29	225	56	106	24.51	17.16	39.60
21	A	27.1	3.9	4.52	0.22	0.3	47.9	18	112	67	771	23.38	18.36	36.71
426	A	28	4.81	0.38	0.68	0.7	44.1	46	249	94	107	22.20	15.53	43.85
407	A	25.1	2.99	4.45	0.42	0.5	51.7	15	160	57	599	22.10	17.94	32.81
20	A	24.6	3.02	3.94	0.49	0.9	52.9	10	177	43	590	21.24	17.31	32.14
257	A	24.9	3.35	1.91	0.41	0.7	54.4	20	187	50	291	21.23	17.13	34.06
482	A	25.7	3.67	0.07	0.24	0.6	52.2	27	198	80	1	20.91	14.40	40.68
19	A	23.2	2.56	4.44	0.26	0.4	56.1	18	152	40	593	20.88	17.81	30.13
206	A	23.7	3.11	1.12	0.18	0.2	58.5	20	127	81	892	20.79	16.63	33.36
258	A	25.2	4.13	1.99	0.55	0.9	52.2	11	270	61	270	20.67	17.09	34.35
18	A	22.5	3.03	3.65	0.28	0.1	57.5	18	180	49	647	20.49	17.86	29.60
82	A	22.9	3.07	5.06	0.25	0.4	53.6	16	160	59	902	20.20	18.04	30.64
908	A	21.8	1.9	4.24	0.24	0.6	55.7	90	168	62	724	19.99	17.43	29.36
255	A	23.4	3.6	2.51	0.42	0.6	51.1	7	180	64	571	19.79	17.34	32.87
430	A	24	3.63	0.25	0.57	0.5	53.7	32	190	68	87	19.74	15.10	36.75
109	A	23.2	4.03	1.54	0.84	0.2	51.5	16	216	82	575	19.64	16.90	34.12
453	A	21.5	2.59	3.97	0.18	0.4	54.9	21	106	56	653	19.44	18.25	28.68
55	A	22.6	3.32	3.71	0.5	0.6	52.5	19	171	76	580	19.40	17.53	30.92
56	A	22.2	3.34	3.26	0.49	0.5	55.5	70	154	69	591	19.09	17.48	30.29
54	A	22.4	3.34	3.71	0.55	0.7	56.4	32	134	72	605	19.09	17.30	29.42
184	A	19.5	0.46	4.45	0.15	0.7	69.3	6	81	1	1696	19.03	15.92	21.99

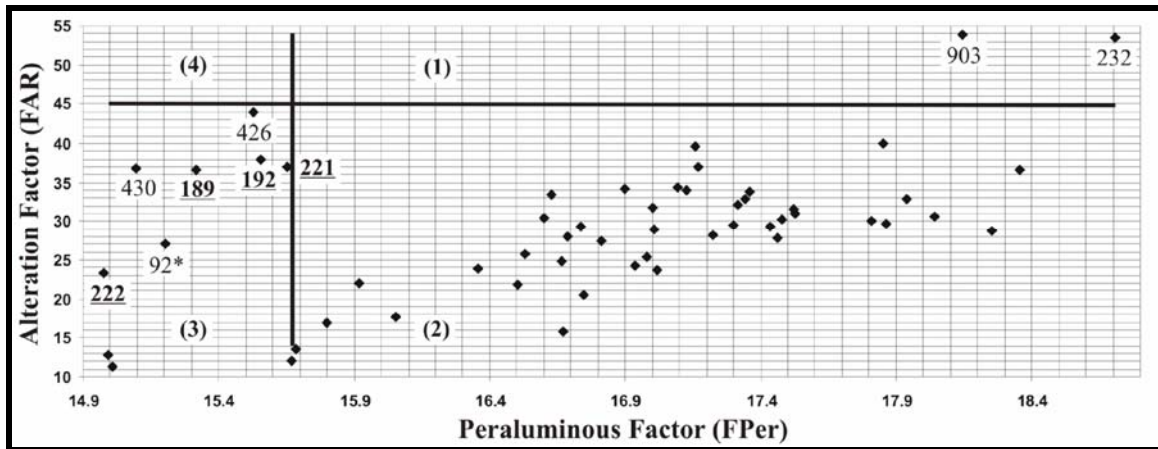


**Figure 5.4:** The peraluminous factor (FPer) versus alteration factor (FAR), regional data set [189]:  $MgO \gg K_2O$ ; 92\*, 426 and 430:  $MgO > K_2O$  from different areas; 903 and 232: very high  $Al_2O_3$ .

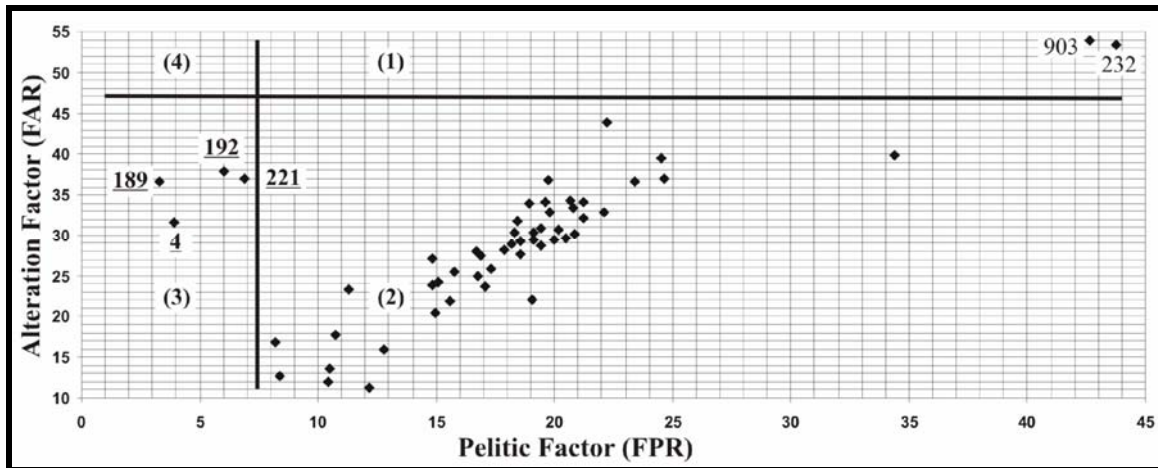


**Figure 5.5:** The pelitic factor (FPR) versus alteration factor (FAR), regional data set [189]:  $MgO \gg K_2O$ ; 903: very high  $Al_2O_3$ .

The amphibolite and peraluminous data set are ranked based on peraluminous factor (FPer) values, and the results are given in Table 5.4. In order to identify amphibolite samples that were possible affected by the alteration process and thereby attaining peraluminous characteristics, the variation of the peraluminous factor versus amphibolite factor is shown in Figure 5.6. All the peraluminous rocks are located in the fourth quarter of the figure and have peraluminous factor values  $> 3$ , and amphibolite factor values  $< 2.5$ . Four samples (232, 903, 453 and 21) have the highest values for the peraluminous factor ( $> 7$ ). Amphibolite samples are situated in the second, third and fourth quarter. Only one of these samples (sample 791), which plot in the fourth quarter, has a slightly



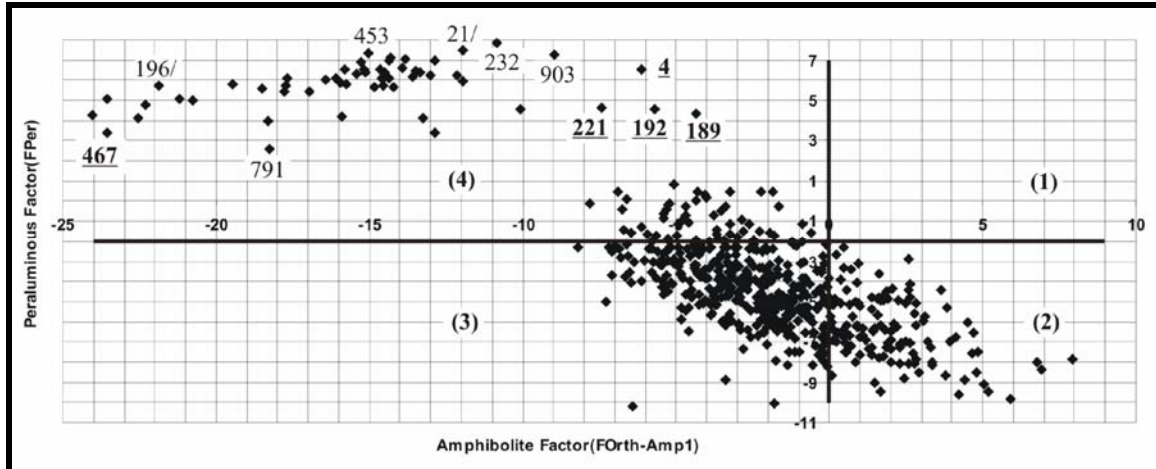


**Figure 5.6:** The peraluminous factor (FPer) versus amphibolite factor (FOrth-Amp1) for the regional data set [**189**: MgO>>K<sub>2</sub>O; 196/, 453 and **467**: K<sub>2</sub>O>MgO from different areas; 903 and 232: very high Al<sub>2</sub>O<sub>3</sub>; 791: high Na<sub>2</sub>O and CaO contents].

higher peraluminous value (2.5). The remained amphibolite samples display low peraluminous factor values (<1).

The variations of ortho-amphibolite factors (Foa1) versus para-amphibolite factors (Fpa3) are plotted in Figure 5.7. In general, the para-amphibolites have a para-amphibolite factor similar to the peraluminous rocks. This is because the precursors of the para-amphibolites represent a sedimentary mix of shale and carbonate material. Ortho-amphibolites have para-amphibolite factor values lower than -100. Peraluminous samples are shown together with amphibolite samples in this diagram. The peraluminous rocks in this figure are situated in the third quarter and have an ortho-amphibolite factor of less than -8.5. Again only sample (791), which plots in the peraluminous field, has a slightly higher peraluminous values (2.5). There is an amphibolite sample (196), which has a very low para-amphibolite factor value (<-300), with an ortho-amphibolite factor value of less than -8.5. This sample is completely separated from peraluminous field. The rest of the amphibolite samples have para-amphibolite factors higher than -8.5 and are located in the first, second, third and fourth field.

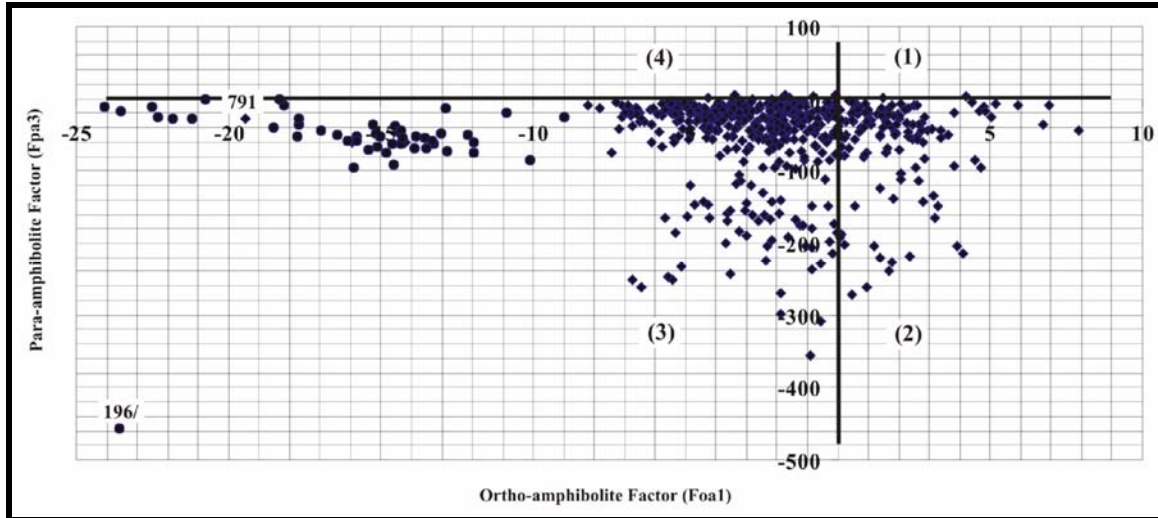


**Figure 5.7:** The para-amphibolite factor ( $F_{para-amp3}$ ) versus ortho-amphibolite factor ( $F_{ortho-amp1}$ ), regional amphibolite and peraluminous data set [diamond filled: peraluminous and square filled: amphibolite].

Figure 5.8 shows the variation of the general factor for amphibolite ( $F_{Amp2}$ ) versus the para-amphibolite factor ( $F_{Para-Amp3}$ ) for amphibolite samples. Assumed para-amphibolite samples have higher values of the para-amphibolite factor and the assumed ortho-amphibolite samples have low values of para-amphibolite factor. Amphibolite samples in this diagram are situated in the first and second field. It is expected that the discrimination between these amphibolite types could be improved if samples were also analysed for Ni (Leake 1964) and Sc (Theart 1985).

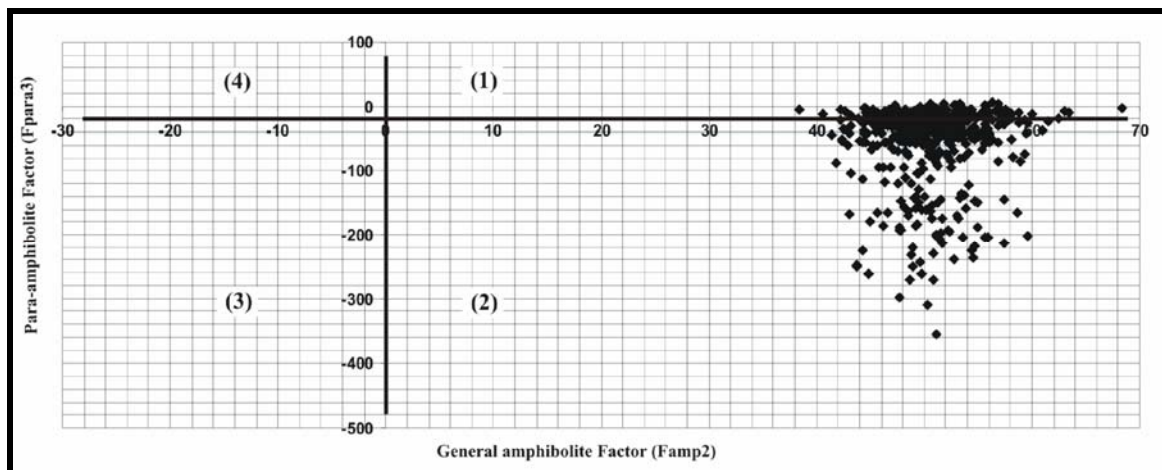


**Figure 5.8:** The para-amphibolite factor ( $F_{para-amp3}$ ) versus general amphibolite factor ( $F_{amp2}$ ) for the regional amphibolite data set.



Similarly, to identify biotite-hornblende-gneiss samples that were potentially affected by the alteration process, the biotite-hornblende-gneiss factor values are compared with values for the peraluminous factor. Values calculated for the biotite-hornblende-gneiss and peraluminous factors are listed in Table 5.5. These values were calculated for a combined data file consisting of biotite-hornblende-gneiss and peraluminous samples. The variation in the biotite-hornblende-gneiss factor versus peraluminous factor is shown in Figure 5.9. All the biotite-hornblende-gneiss samples plot outside the field defined by the peraluminous samples and no distinctly anomalous samples could be identified. However, a large number of the biotite-hornblende-gneiss samples plots close to the peraluminous dividing line of 3, based on the peraluminous factor.

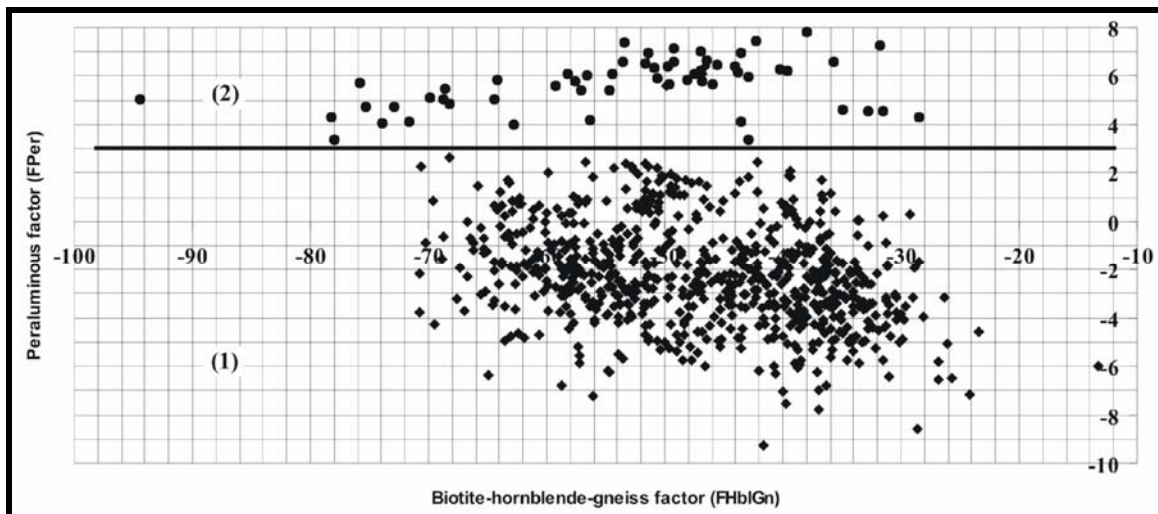


**Figure 5.9:** Biotite-hornblende-gneiss factor (FHbl-Gn) versus peraluminous factor (FPer), combined data set of biotite-hornblende-gneiss and peraluminous samples, regional data set [diamond filled: peraluminous and square filled: biotite-hornblende-gneiss samples].



In the same way, to identify leucogneiss samples that were potentially affected by the alteration process, the leucogneiss factor values are compared with values for the peraluminous factor. Values calculated for the leucogneiss and peraluminous factors are listed in Table 5.6. Figure 5.10 shows the variation of the leucogneiss factor versus peraluminous factor in a data file that includes both peraluminous and leucogneiss rocks. Leucogneiss samples are located in the second field and their peraluminous factor is less than 4. The leucogneiss factor values for these samples are higher than peraluminous samples and vary from 40 to 90. Peraluminous samples in this diagram are located in the first field, where the peraluminous factor is greater than 4. The leucogneiss factor values of peraluminous rocks vary from 7 to 72. However, some of the leucogneiss samples plot close to the peraluminous dividing line of 4, defined above.

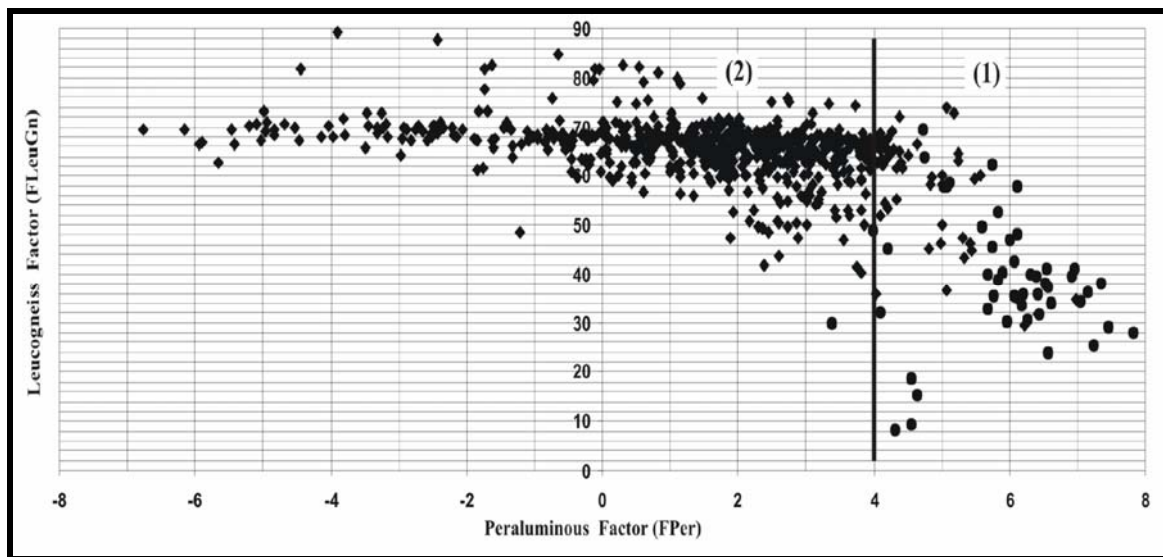


**Figure 5.10:** The leucogneiss factor (FLeu-Gn) versus peraluminous factor (FPer), mixed of peraluminous and leuco-gneissic samples, regional data set [diamond filled: peraluminous and square filled: leucogneiss samples].



Factor analyses were used in the above paragraphs to identify rocks from the regional data set that were possibly affected by hydrothermal processes related to sulphide mineralization processes. In the following section various techniques will be used to prioritize potential target areas for follow-up exploration.

### **5.6. Prioritization of the anomalous samples in the regional data set**

The objective with an initial geochemical exploration survey is to identify anomalous areas or probable mineralized zones for follow up exploration. When there is more than one such anomalous area, these should be ranked based on the calculated relative potential for all the samples. For this purpose, a data file composed of the peraluminous, pelitic and alteration factor values was used in a maximum likelihood procedure to identify anomalous sub-populations.

A cumulative frequency probability plot of the alteration factor values is used to identify estimates of the anomalous sub-population. The probplot software requires positive variable values, and for this reason a constant value was added to all factors returning same negative values. This results a shift in the data without any influence on the underlying distribution of the values.

The cumulative frequency probability plot of the regional data set is shown in Figure 5.11 for the alteration factor. The observed distribution may be described as a mixture of three sub-populations. The first represents less than 1.2% of the values, the second represent between 1.2% and 53.7% of the values and the third comprise more than 53.7% of the values. The anomalous sub-population has a lower threshold for the alteration factor values of 17.82 (Table 5.7), and 975 samples return of greater than this. These samples were separated from the whole data set (2016 samples in total), and the alteration factor values were recalculated using the SAS software. The resulting subset was again inspected and the probability plot results are shown in Figure 5.12. Again three sub-populations are identified based on this diagram. 1% of the data belongs to the first, the

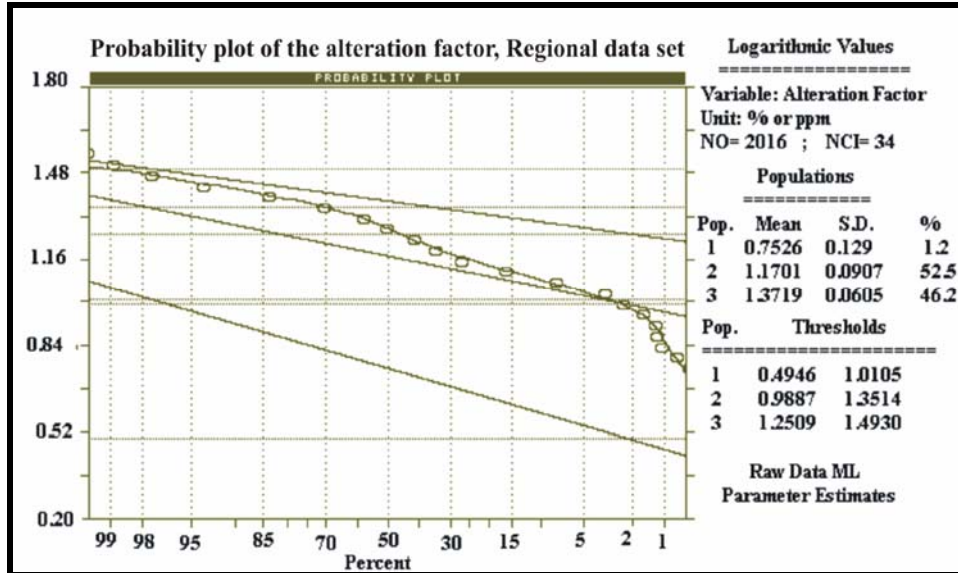


Figure 5.11: The probability plot of whole regional data set for the alteration factor (FAR).

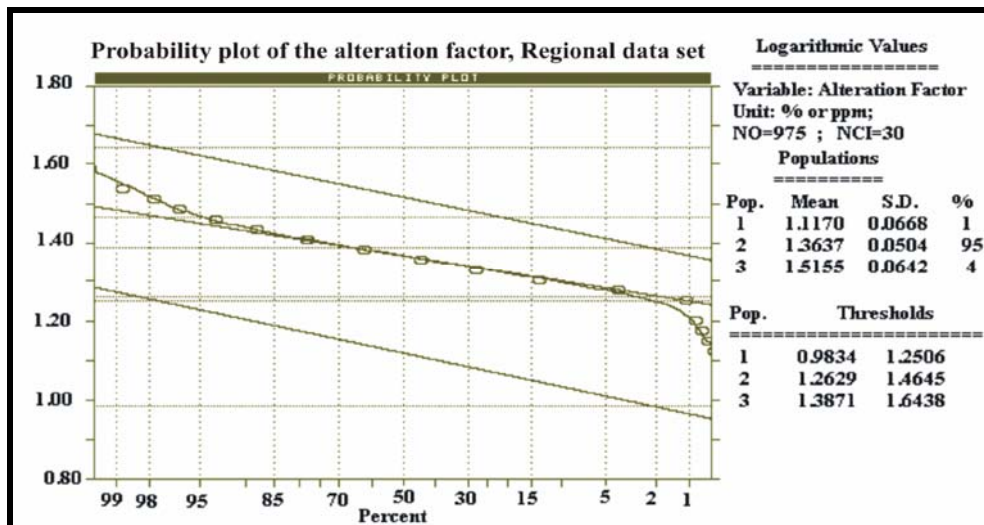


Figure 5.12: The probability plot of anomalous values of the last stage for the alteration factor (FAR), regional data set.

second consists of between 1 and 96%, and the third contains the upper 4% of the data. The descriptive statistics of the anomalous sub-populations thus identified are listed in Table 5.8. Based on the new threshold value of the alteration factor (29.1), 57 samples are identified as anomalous and are listed with their respective coordinates in Table 5.9.

**Table 5.7:** The threshold value for each factor, regional data set (n= 2016 samples).

Factor	No. of popul.	Means (M)	Std. Dev. (SD)	%	Threshold values
FPer	1	5.9	-4.6 +7.6	16.5	3.6 9.9
	2	9	-7.7 +10.5	44.6	6.6 12.3
	3	13.8	-12.2 +15.7	39	10.8 17.8
FAR	1	5.7	-4.2 +7.6	1.3	3.1 10.2
	2	14.8	-12 +18.2	52.5	9.7 22.5
	3	23.5	-20.5 +27.1	46.2	17.8 31.1
FPR	1	7.1	-3.9 +13.1	9.8	2.1 24.1
	2	12.956	-10.7 +15.7	90.2	8.8 19
FAmp <sub>2</sub>	1	14.3	-10 +20.5	40.2	6.9 29.5
	2	32.600	-27 +39.3	25.5	22.4 47.4
	3	48.3	-43.3 +53.8	34.3	38.8 60
FGn	1	28.2	-22.4 +33.9	36	19.4 40.8
	2	51.1	-41.7 +62.6	38.7	34.1 76.7
	3	66.2	-63.2 +69.4	25.3	60.3 72.7

Note: No. of popul.: Number of population, Std. Dev.: Standard deviation (SD)

**Table 5.8:** The threshold value for peraluminous and alteration factors, regional data set (n= 975 samples).

Factor	No. of population	Means (M)	Std. Dev. (SD)	%	Threshold values
FAR	1	13	-11.2 +15.3	1	9.6 17.8
	2	23	-20.6 +25.9	95	18.3 29.1
	3	32.8	-28.3 +38	4	24.4 44
FPer	1	4.5	-3.4 +6	7.7	2.5 8.1
	2	8.3	-6.6 +10.6	85.7	5.2 13.4
	3	16.9	-15 +17	6.6	13.3 21.5

Note: No.: Number, Std. Dev.: Standard deviation (SD)

Samples identified in the previous sections showing features that could be related to the hydrothermal alteration, are identified by the Code “A” in Tables 5.1 to 5.6 and 5.9. As can be seen, most of the samples in Table 5.9 were given the Code “A”. However, some of these may now be excluded where the samples returned K<sub>2</sub>O contents higher than the MgO contents, as these rocks probably had common shale precursors. It was also shown in section 5.5 that para-amphibolites show high peraluminous factors values. These samples could be discarded using their high CaO and K<sub>2</sub>O and low MgO contents. Para- and ortho-amphibolites are identified with the Codes “C1” and “C2” respectively in Table 5.9. The remaining 15 samples from the original 57 samples in this subset (Table 5.9) may be regarded as highly anomalous and should be given priority for follow-up exploration.

The high priority samples include four samples (4, 189, 192, and 221) which have extremely high MgO and low K<sub>2</sub>O contents, eleven samples (482, 430, 426, 206, 255, 256, 257, 258, 77, 109 and 531) with MgO higher than K<sub>2</sub>O. In addition, some of these samples have anomalous Zn concentrations (180-349 ppm).



**Table 5.9:** The sample numbers and localities for anomalous samples with selected chemical data.

No.	Code	Pr.	CaO	Na <sub>2</sub> O	Al <sub>2</sub> O <sub>3</sub>	MgO	K <sub>2</sub> O	SiO <sub>2</sub>	Cu	Zn	Ni	%AI	%CCPI
54	A		0.55	0.7	22.4	3.34	3.71	56.4	32	134	72	84.94	88.18
55	A		0.5	0.6	22.6	3.32	3.71	52.5	19	171	76	86.47	89.98
56	A		0.49	0.5	22.2	3.34	3.26	55.5	70	154	69	86.96	90.76
74	A		0.56	0.8	28.4	2.97	3.67	48.4	21	207	53	83.00	89.34
77	A	*	0.31	0.6	29.1	3.94	1.51	47.9	29	225	56	85.69	94.91
82	A		0.25	0.4	22.9	3.07	5.06	53.6	16	160	59	92.60	86.76
109	A	*	0.84	0.2	23.2	4.03	1.54	51.5	16	216	82	84.27	96.38
232	A		0.1	0.7	47.3	1.1	5.19	36.3	11	134	22	88.72	71.30
903	A		0.78	0.1	45.5	1.41	2.76	37.7	12	175	28	82.57	89.50
908	A		0.24	0.6	21.8	1.9	4.24	55.7	90	168	62	87.97	87.82
338	A		0.22	0.8	36.7	0.74	7.68	42.2	19	40	14	89.19	55.87
407	A		0.42	0.5	25.1	2.99	4.45	51.7	15	160	57	89.00	87.64
255	A	**	0.42	0.6	23.4	3.6	2.51	51.1	7	180	64	85.69	93.01
256	A	**	0.45	0.6	23.1	4.27	2	53	74	159	75	85.66	94.71
257	A	**	0.41	0.7	24.9	3.35	1.91	54.4	20	187	50	82.57	93.55
258	A	**	0.55	0.9	25.2	4.13	1.99	52.2	11	270	61	80.85	93.09
421	A		0.73	0.7	21.2	2.87	3.02	53.2	13	173	67	80.46	91.95
426	A	**	0.68	0.7	28	4.81	0.38	44.1	46	249	94	79.00	88.25
206	A	**	0.18	0.2	23.7	3.11	1.12	58.5	20	127	81	91.76	96.47
482	A	**	0.24	0.6	25.7	3.67	0.07	52.2	27	198	80	81.66	98.60
430	A	**	0.57	0.5	24	3.63	0.25	53.7	32	190	68	78.38	98.38
68	B		1.1	1.2	18.7	3.52	0.62	58	14	177	82	64.29	96.16
443	C <sub>1</sub>		23.3	0.2	23.6	1.12	0.07	38.9	14	41	21	4.82	98.68
785	C <sub>1</sub>		16.6	0.9	22	1.42	0.29	46.2	70	40	19	8.90	96.54
896	C <sub>1</sub>		13.3	1.7	22.6	2.79	0.87	48.2	45	132	33	19.61	91.71
18	A		0.28	0.1	22.5	3.03	3.65	57.5	18	180	49	94.62	89.25
19	A		0.26	0.4	23.2	2.56	4.44	56.1	18	152	40	91.38	86.58
20	A		0.49	0.9	24.6	3.02	3.94	52.9	10	177	43	83.35	87.70
21	A		0.22	0.3	27.1	3.9	4.52	47.9	18	112	67	94.18	89.57
326	C <sub>2</sub>		11.5	0.5	16	3.4	0.12	47.6	12	44	28	22.68	99.01
365	C <sub>2</sub>		17.4	0.7	23.4	2.25	0.17	45.3	17	72	20	11.79	97.13
461	C <sub>2</sub>		16.5	0.9	23.5	0.77	0.1	48.8	26	13	9	4.76	95.94
495	C <sub>2</sub>		13.1	0.7	22.4	4	0.26	44.5	12	10	71	23.59	97.79
506	C <sub>2</sub>		15.5	1	23.4	3.7	1.03	40.6	15	46	34	22.28	95.06
526	C <sub>1</sub>		15.9	0.9	21.5	3.56	0.73	44.8	12	61	261	20.34	95.70
536	C <sub>2</sub>		21.5	0.4	25	1.8	0.19	37.6	17	52	22	8.33	98.32
586	C <sub>2</sub>		13.7	2.5	19.4	2	0.62	44.5	10	138	21	13.92	93.66
624	C <sub>2</sub>		12.9	0.7	20.2	5.3	0.23	48.7	100	58	29	28.91	97.50
641	C <sub>2</sub>		21.2	0.4	23.7	2.5	0.05	42.3	21	22	33	10.56	98.36
737	C <sub>2</sub>		19	0.6	22.7	1.4	0.34	43.7	14	39	21	8.15	96.96
748	C <sub>2</sub>		15.2	1.8	23.7	1.63	0.23	47.2	22	49	14	9.86	93.02
750	C <sub>2</sub>		15.8	1.3	21.1	2.9	0.19	44.6	40	79	14	15.30	96.28
88	C <sub>2</sub>		15.9	0.7	19.2	5.92	0.62	41.5	21	161	91	28.26	97.15
4	A	***	0.32	0.3	16.5	15	0.97	48.5	15	177	50	96.26	98.11
531	A	*	0.22	0.5	21.9	3.57	2.21	55.7	80	204	69	88.92	93.98
53	A		0.29	0.9	21.6	2.87	3.85	56.7	25	151	57	84.96	88.31
221	A	***	0.45	0.6	16.6	10.7	0.07	45.8	14	167	88	91.12	99.15
189	A	***	0.84	0.6	15.5	13.7	0.23	41	12	349	25	90.63	99.08
192	A	***	0.43	0.3	16.2	11.7	0.24	43	17	178	24	94.24	99.40
20	C <sub>2</sub>		9.96	1.1	16.9	7.08	0.18	45.9	28	99	22	39.63	97.72
157	C <sub>1</sub>		20.8	0.6	24.7	0.41	0.8	43.2	14	0	9	5.35	94.99
226	C <sub>1</sub>		13.8	1.2	24.9	1.38	1.77	45.1	6	20	5	17.36	89.17
290	C <sub>2</sub>		10.6	1.4	15.5	5.03	0.37	46.3	71	107	22	31.03	97.12
381	C <sub>1</sub>		22.2	0.4	23.2	1.8	0.2	41.6	7	42	8	8.13	97.49
468	C <sub>2</sub>		13.3	1.8	22.1	3.95	0.28	48.5	198	46	34	21.88	93.43
523	C <sub>2</sub>		14.2	0.8	23.2	5.79	1.38	41.1	7	70	37	32.34	94.35
526	C <sub>1</sub>		18.3	1.5	22.5	0.49	0.2	46.4	1	12	4	3.37	94.09

Pr.: Prioritised anomaly (\*=moderately high; \*\*=high and \*\*\*= very high)

The alteration index and CCPI were calculated in Table 5.9, and the box plot is shown in Figure 5.13 (see Appendix A, Figure A.6 for more detail). Peraluminous samples with high Mg ( $MgO > K_2O$ ) have  $AI > 64\%$  and  $CCPI > 93\%$ , but peraluminous samples with high K ( $K_2O > MgO$ ) have  $55\% < CCPI < 93\%$  with the same amount of AI. The rest of the samples have  $AI < 40\%$  and  $CCPI > 88\%$ .

The probability plot based on data in Table 5.9 for Zn, Cu and Ni contents is shown in Figures 5.14 to 5.16. The distribution of the data as can be seen in the probability plots can best be modelled as a mixture of three sub-populations by using maximum likelihood procedure. Three sub-populations are identified for Zn (Fig. 5.14). 50.2% of the data belong to the first, the second consists 14.7% of the data and the third contains 35.1% of the data. The anomalous sub-population has Zn values higher than approximately 240 ppm (Table 5.10, two times the lower level of the threshold of the last sub-population).

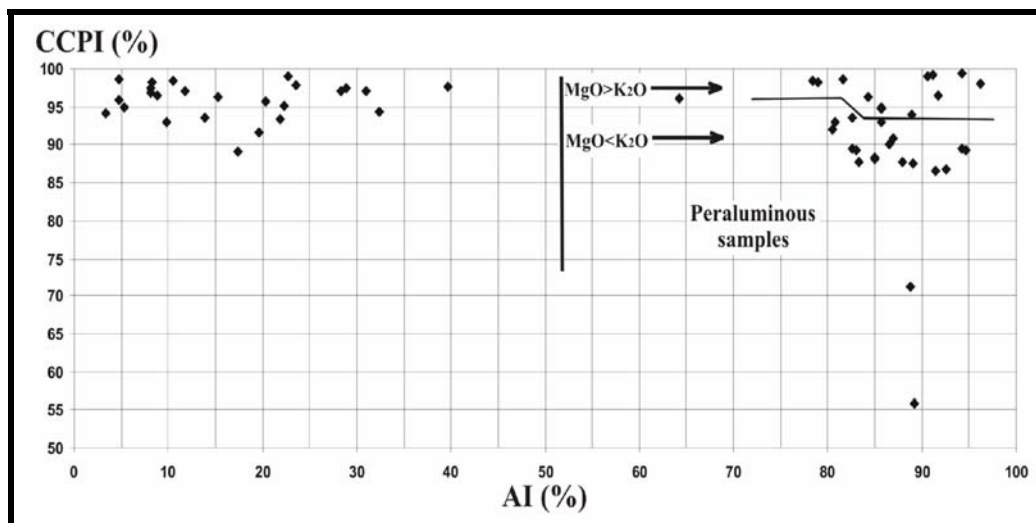


Figure 5.13: Box plot of the final results for the regional data set.

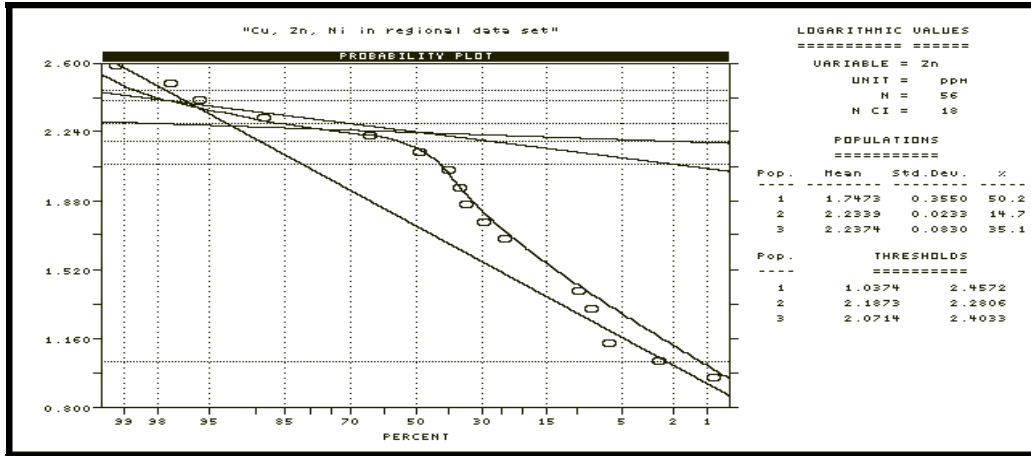


Figure 5.14: The probability plot of Zn contents based on the data in Table 5.9, regional data set.

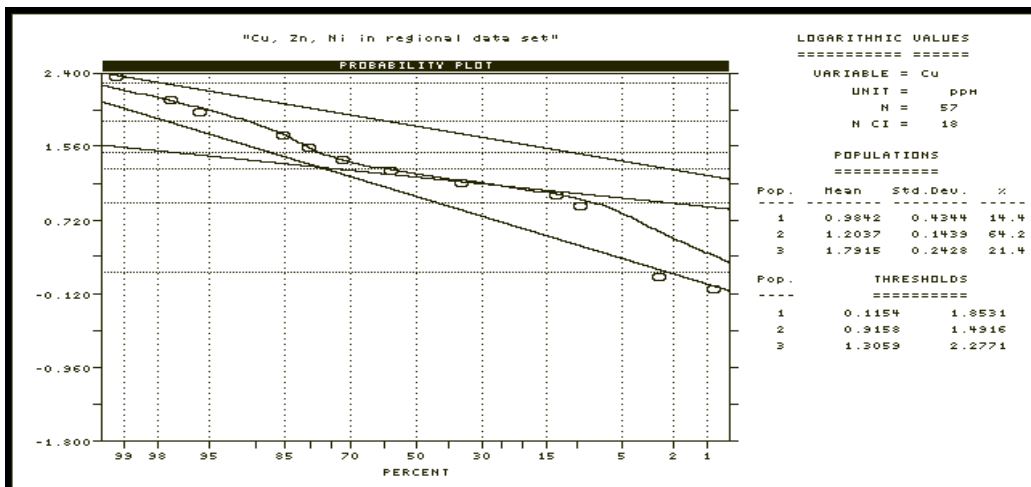


Figure 5.15: The probability plot of Cu contents based on the data in Table 5.9, regional data set.

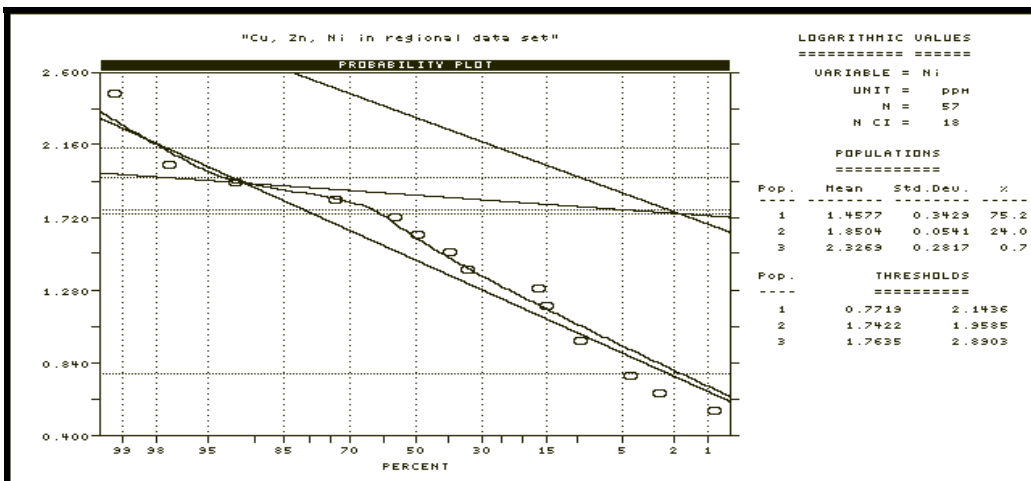


Figure 5.16: The probability plot of Ni contents based on the data in Table 5.9, regional data set.

**Table 5.10:** The threshold value for Zn, Cu and Ni, regional data set (n= 57 samples).

Factor	No. of population	Means (M)	Std. Dev. (SD)	%	Threshold values
Zn	1	56	-24.7 +126.6	50.2	11 287
	2	171	-162.4 +180.8	14.7	154 191
	3	173	-142.7 +209.1	35.1	118 253
Cu	1	10	-3.6 +26.2	14.4	1 71
	2	16	-11.5 +22.3	64.2	8 31
	3	62	-35.4 +108.2	21.4	20 189
Ni	1	29	-13 +63.2	75	6 139
	2	71	-62.6 +80.3	24	55 91
	3	212	-111 +406.1	1	58 777

Note: No.: Number, Std. Dev.: Standard deviation (SD)

Three sub-populations are identified for Cu (Fig. 5.15). The first of these sub-populations contains less than 14.4% of the samples, the second between 14.4% and 78.6% and the third 21.4% of the data. The anomalous sub-population has Cu concentrations higher than 40 ppm (Table 5.10, two times the lower level of the threshold of the last sub-population).

Three sub-populations are identified for Ni (Fig. 5.16). The first includes 75% of the data, the second consists 24% of the data and the third 1% of the data. The anomalous sub-population has Ni contents higher than 116 ppm (Table 5.10, two times the lower level of the threshold of the third sub-population).

Based on the threshold values for Zn, Cu and Ni and Table 5.9, Ni distributions were found to be not as diagnostic as is that of Zn and Cu, which may be used as a vector in the prioritization of anomalous areas.

MgO and K<sub>2</sub>O contents, peraluminous ratio, AI, CCPI, FPer and FAR are used to rank the anomalous values in Table 5.11. The rocks in the alteration zone of VHMS metamorphic deposits are peraluminous or the peraluminous factor has the highest values. This zone may be recognized by MgO higher (to extremely higher) than K<sub>2</sub>O or the highest alteration factor values. Alteration index and CCPI have the highest values in the alteration pipes of VHMS deposits. These characteristics are used with the data in Table 5.11 and to prioritize the anomalous values. In the last column of this table, the anomalies are ranked.

The geology of the northern part of the Areachap Group, of the eastern Namaqua Metamorphic Province is given in Figure 5.17. Four Cu-Zn-Pb mineralized occurrences are indicated to the south of Upington on the geological map by the Council for Geoscience (2820 Upington 1:250000 Geological Series).

Four anomalous areas identified during this study in the research area. Two of these anomalies are prioritized as rank one on the anomaly map, which has extremely high MgO and low K<sub>2</sub>O contents. The other two anomalies are prioritized as rank two, which have MgO>K<sub>2</sub>O. Anomalies that are prioritized as rank three and have MgO>K<sub>2</sub>O include of only one sample.

The variation of the alteration factor for some of these prioritised areas, rank one and two, may now be represented in traverses. The traverse of the anomalous area of rank one is shown in Figure 5.18 and that of rank two in Figure 5.19. These two traverses show the location of values higher than threshold value, determined with the probe plot procedure (Sinclair, 1976).



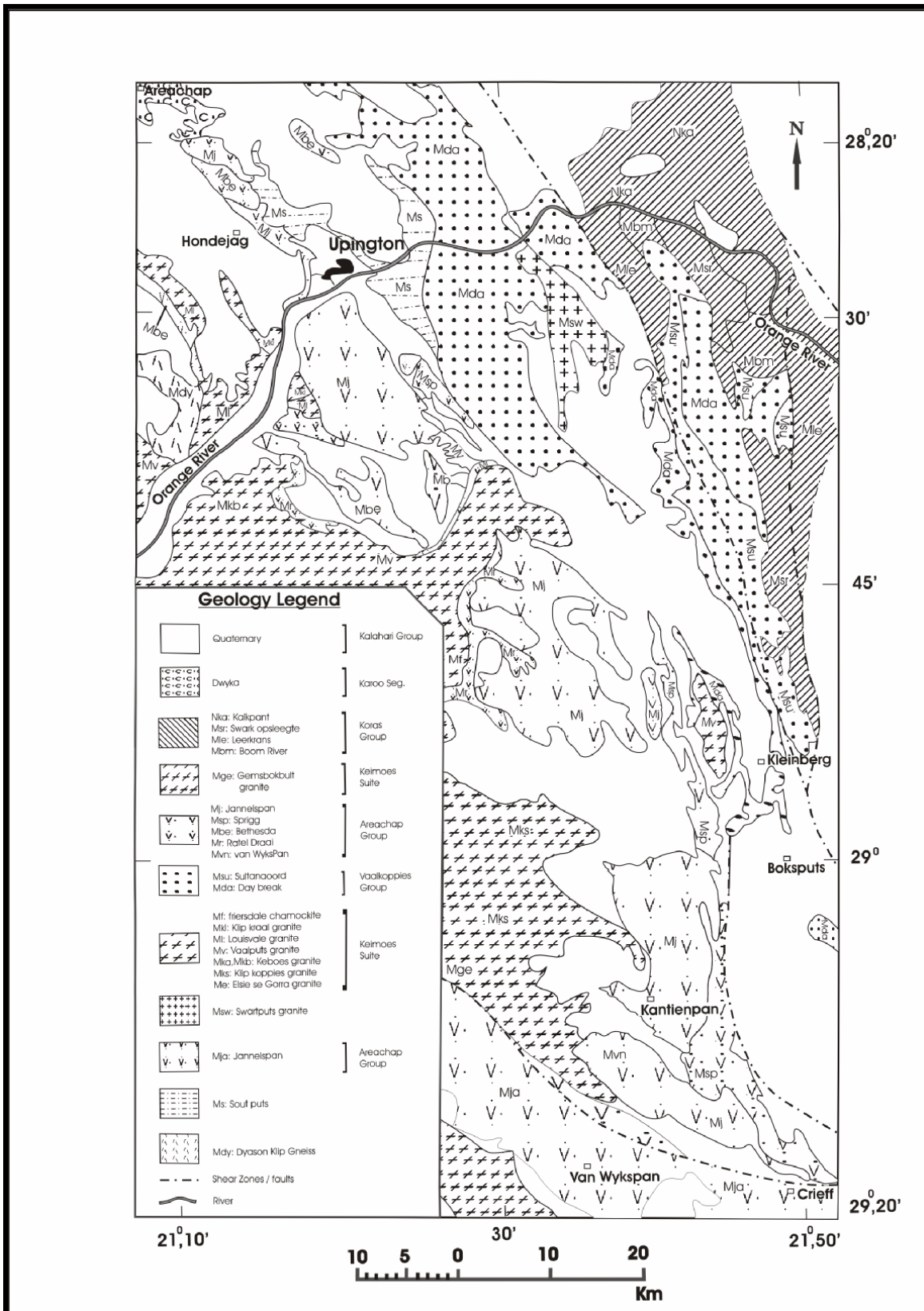


Figure 5.17: Geology of the northern part of the Areachap Group, eastern Namaqua Province.

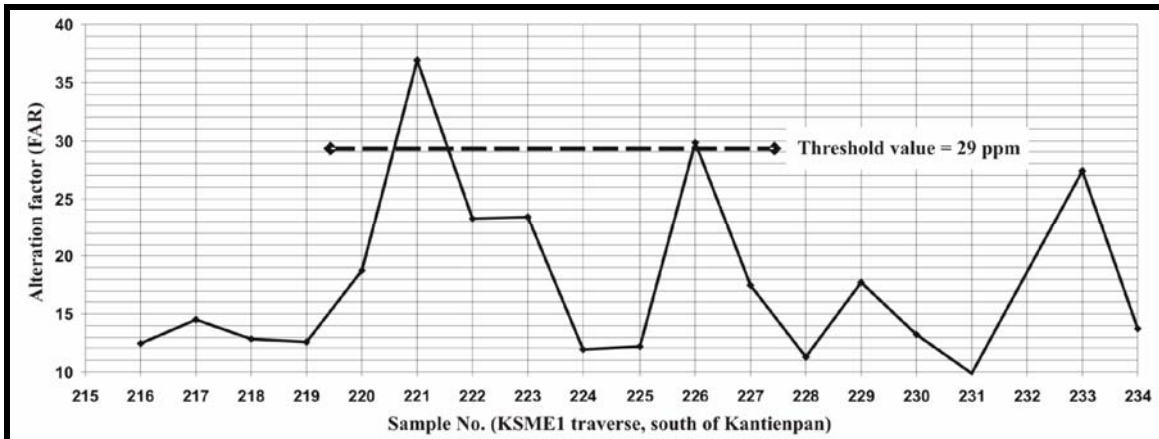


Figure 5.18: The alteration factor versus sample number in-prioritised Traverses, rank one.

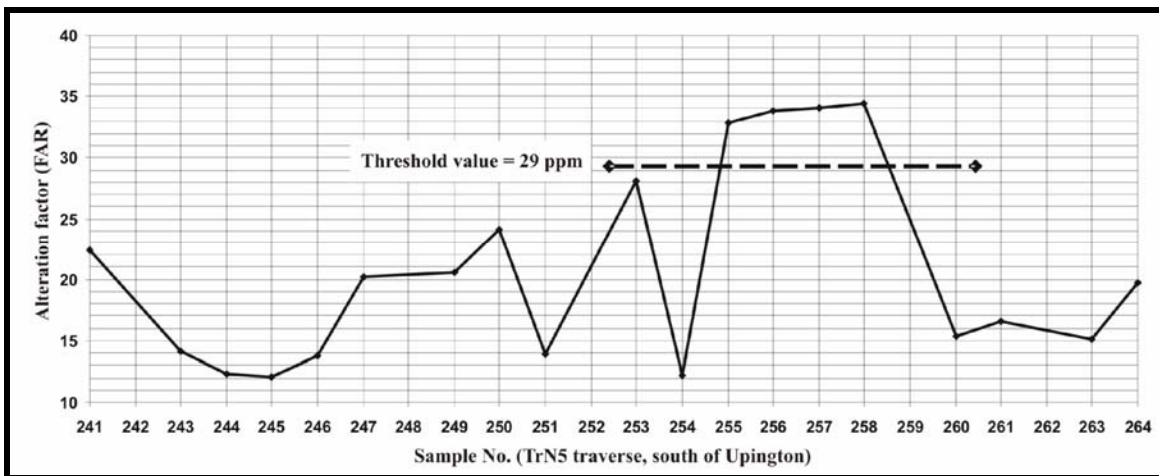


Figure 5.19: The alteration factor versus sample number in-prioritised traverses, rank two.



